

Characterization of Vps41 Subunit of Mammalian HOPS Complex

Arsila Ashraf P.K

*A dissertation submitted for the partial fulfilment of
BS-MS dual degree in Science*



Indian Institute of Science Education and Research Mohali
April 2016

*Dedicated to my mother, brothers Abdu and Abi, friends and
teachers for their valuable love and support*

*“We are all a little broken. But last time I checked **broken crayons still color the same**”*

-Trent Shelton

Certificate of Examination

This to certify that the dissertation entitled “**Characterization of Vps41 Subunit of Mammalian HOPS Complex**” submitted by Ms. Arsila Ashraf P.K (MS11068) for the partial fulfilment of BS-MS dual degree programme of the Institute, has been examined by the thesis committee duly appointed by the Institute. The committee finds the work done by the candidate satisfactory and recommends that the report be accepted.

Dr. Mahak Sharma
(Supervisor)

Dr. Samarjit Bhattacharya
(Committee Member)

Dr. Kausik Chattopadhyay
(Committee Member)

Dated: April 20, 2016

Declaration

The work presented in this dissertation has been carried out by me under the guidance of Dr. Mahak Sharma at the Indian Institute of Science Education and Research Mohali.

This work has not been submitted in part or in full for a degree, a diploma, or a fellowship to any other university or institute. Whenever contributions of others are involved, every effort is made to indicate this clearly, with due acknowledgement of collaborative research and discussions. This thesis is a bonafide record of original work done by me and all sources listed within have been detailed in the bibliography.

Arsila Ashraf P.K

(Candidate)

Dated: April 20, 2016

In my capacity as the supervisor of the candidate's project work, I certify that the above statements by the candidate are true to the best of my knowledge.

Dr. Mahak Sharma

(Supervisor)

Acknowledgement

I am highly indebted to my supervisor Dr. Mahak Sharma for hiring me to work with her. I sincerely thank her for the guidance and constant supervision throughout this project. I am filled with gratitude towards her for her support, inspiration, advices, and continuous motivation and for being a great mentor. I would also like to thank her for spending valuable time in my times of need.

I would like to thank my PhD guide Divya Khatter for her guidance and motivation in carrying out the project. I would also like to thank the other lab members; Aastha Sindhwani for her love and care, Devashish Dwivedi for his critical suggestions, Rituraj Marwaha for being a good teacher, Divya Jagga for her generosity and Partha Sankar R.P.S for his immense love, care and support. Special thanks to Aastha and Devashish for teaching me Confocal Microscopy.

I extend my sincere thanks to all the 3TL2 lab members, especially Bhupinder Singh and Ankita Das for their support and for being great friends. I also thank all the faculty and staffs of Department of Biological Sciences and IISER Mohali for creating a great vibrant environment to learn and conduct research.

From the bottom of my heart, I sincerely thank my mother for being a great woman and moreover my best friend. I thank her for her unconditional love and support, for her trust and belief in me and for pushing me to explore limitless in life. I thank my sweet younger brothers Abdu and Abi for the beautiful times together and for pestering me with questions, love and care.

And I would like to thank my precious jewels, Azam, Molu, Shibil, Partha, Deepthi, Manu, Jopaul, Aiswarya, Anjali, Thapasya, Anooja and Tess for the love, hate, fights, fun and adventure. I thank Azra Fazal and Majidha Abdulla for being so awesome and beautiful sisters. I thank all of them wholeheartedly for making my life beautiful and for being around during my difficult times.

Finally, I thank the Almighty God for the special people around me, good and bad things in my life and for my wonderful life.

List of Figures

Figure 1: **Intracellular pathways to the lysosome**

Figure 2: **A detailed schematic representation of endo-lysosomal pathway**

Figure 3: **Schematic representation of CORVET and HOPS function within the endo-lysosomal pathway**

Figure 4: **Model of eukaryotic HOPS tethering complex**

Figure 5: **Function of HOPS complex**

Figure 6: **Vps41 subunit of HOPS complex localizes to the lysosomes**

Figure 7: **Domain architecture of Vps41 subunit of HOPS complex**

Figure 8: **Co-immunoprecipitation of Vps18 by Vps41**

Figure 9: **Representation of Zinc metal binding in RING domain**

Figure 10: **Domain architecture of Vps41 depicting interactions with different partners**

Figure 11: **Yeast two hybrid interaction of Vps41 with Vps18**

Figure 12: **Domain architecture of Vps41 713X mutant and Co-immunoprecipitation analysis of Vps41 713X with Vps18**

Figure 13: **Colocalization study of Vps41 713X domain deletion mutant with Vps18**

Figure 14: **Domain architecture of Vps41 791X mutant and Co-immunoprecipitation analysis of Vps41 791X with Vps18**

Figure 15: Domain architecture of Vps41 839X mutant and Co-immunoprecipitation analysis of Vps41 839X with Vps18

Figure 16: Vps41 RING-H2 domain

Figure 17: Co-immunoprecipitation of Vps41 Δ RING (First 6 Cysteines/ Histidines are mutated) with Vps18

Figure 18: Co-immunoprecipitation of Vps41 Δ C3H (First 4 Cysteines/ Histidines are mutated) with Vps18

Figure 19: Co-immunoprecipitation of Vps41 C791S C794S (First 2 Cysteines are mutated to Serines) with Vps18

Figure 20: Yeast two hybrid interactions of Vps41 and Vps41 C791S C794S with Vps18

Figure 21: Colocalization study of Vps41 C791S C794S mutant with Vps18

Figure 22: GST Pulldown of HA-tagged Vps41 and HA-tagged Vps41 C791S C794S with GST-tagged Arl8b

Figure 23: Co-immunoprecipitation of Vps41 H819R C822S with Vps18

Figure 24: Yeast two hybrid interaction of Vps18 and Vps18 Δ RING with other HOPS subunits tested using pGBKT7/pGADT7 system

Figure 25: Co-immunoprecipitation of Vps18 C853S C856S (First 2 Cysteines are mutated to Serines) with Vps41

Figure 26: Co-immunoprecipitation of Vps18 C870S H872R (First 2 Cysteines are mutated to Serines) with Vps41

Figure 27: **Purified AKTA fractions for MBP-Vps39 and MBP-Vps18**

Figure 28: **The SDS PAGE gel for purified and concentrated MBP-Vps18 and MBP-Vps39 proteins**

Figure 29: **Antibody test for anti MBP-Vps39 and anti MBP-Vps18 proteins**

Figure 30: **Purification of MBP-Vps39 antibody using Protein G coated beads**

Figure 31: **The immunoblot for testing of Rabbit anti MBP-Vps39 synthesized antibody**

List of Table

| |
|--|
| Table 1: Details of cloning performed as part of MS Thesis project work |
|--|

List of Abbreviations

| | |
|-----------------|--|
| 3-AT | : 3-Amino-1, 2, 4-triazole |
| BSA | : Bovine Serum Albumin |
| EDTA | : Ethylenediaminetetraacetic acid |
| EGTA | : Ethylene glycol tetraacetic acid |
| FBS | : Foetal Bovine Serum |
| GST | : Glutathione S-transferase |
| GTP | : Guanine Triphosphate |
| HA | : Hemagglutinin |
| HEPES | : 4-(2-hydroxyethyl)-1-piperazineethanesulfonic acid |
| HRP | : Horseradish Peroxidase |
| IgG | : Immunoglobulin G |
| IPTG | : Isopropyl β -D-1-thiogalactopyranoside |
| LAMP1 | : Lysosomal-associated membrane protein 1 |
| LB | : Luria Broth |
| MBP | : Maltose Binding Protein |
| NP-40 | : Nonyl Phenoxypolyethoxylethanol-40 |
| PBST | : Phosphate Buffered Saline with Tween 20 |
| PFA | : Paraformaldehyde |
| PIPES | : Piperazine-N,N'-bis(2-ethanesulfonic acid) |
| PMSF | : Phenylmethane Sulfonyl Fluoride or Phenylmethylsulfonyl Fluoride |
| SDS PAGE | : Sodium Dodecyl Sulfate-Polyacrylamide Gel Electrophoresis |

Contents

| | |
|----------------------------|-----|
| List of Figures | i |
| List of Table | iv |
| List of Abbreviations | v |
| Abstract | vii |
| 1. Introduction | |
| 1.1 Basic Knowledge | 1 |
| 1.2 Materials and Methods | 8 |
| 2. Summary and Conclusions | |
| 2.1 Results and Discussion | 13 |
| 2.2 Future Prospects | 32 |
| Bibliography | 33 |

Abstract

Eukaryotic cells are constantly exchanging materials within and with their environment. This involves the endocytic pathway, which forms a dynamic and complex network with continuous fusion and fission of vesicles. The key molecules like small GTPases, tethering factors, SNAREs mediate the fusion and fission. Lysosomes are terminal compartments in the cell that receive cargo to be metabolized or degraded from different organelles including late endosomes, autophagosomes or phagosomes. Homotypic fusion and Protein Sorting (HOPS) is a multi-subunit tethering complex conserved from yeast to humans and mediates the fusion of late endosomes with lysosomes. The four subunits Vacuole Protein Sorting (VPS)11, VPS16, VPS18 and VPS33 form the core complex while VPS39 and VPS41 are the accessory subunits of HOPS complex that are involved in recruitment of HOPS complex to the lysosomal membranes. Previous study from our lab has shown that in mammals, Vps41 subunit of the HOPS interacts with the small GTPase Arl8b and thereby recruits it to the lysosomal membrane. Vps41 then recruits the Vps18 subunit of HOPS and further subunit-subunit interactions assemble the HOPS complex on the lysosome in a stepwise manner. We are currently investigating the interaction of Vps41 with Vps18 and the assembly of HOPS complex on the lysosomes. Co-immunoprecipitation studies using the domain deletion mutants of Vps41 suggests that RING-H2 domain of Vps41 is critical for its interaction with Vps18 and further assembly of HOPS complex. Interestingly, point mutations replacing the cysteine and histidine residues within the Vps41RING-H2 domain abrogate the interaction of Vps41 with Vps18 supported by co-immunoprecipitation, yeast two-hybrid and subcellular localization studies. In a nutshell, these results show that RING-H2 domain of Vps41 is essential for the assembly of HOPS complex on lysosomal membrane and consequent fusion of late endosome with lysosomes.

1. INTRODUCTION

1.1 Basic Knowledge

1.2 Materials and Methods

1.1 Basic Knowledge

1.1.1. Lysosomes: Little Organelle, Big Deal

Lysosomes are membrane-bound organelles serving several functions inside a cell that are crucial for a cell's survival. Lysosomes are specialized compartments for the degradation of endocytosed and intracellular material and essential regulators of cellular homeostasis (Meel and Klumperman 2008). It takes in diverse cargos from different feeder pathways like autophagic, endocytic and phagocytic pathway (shown in Figure 1).

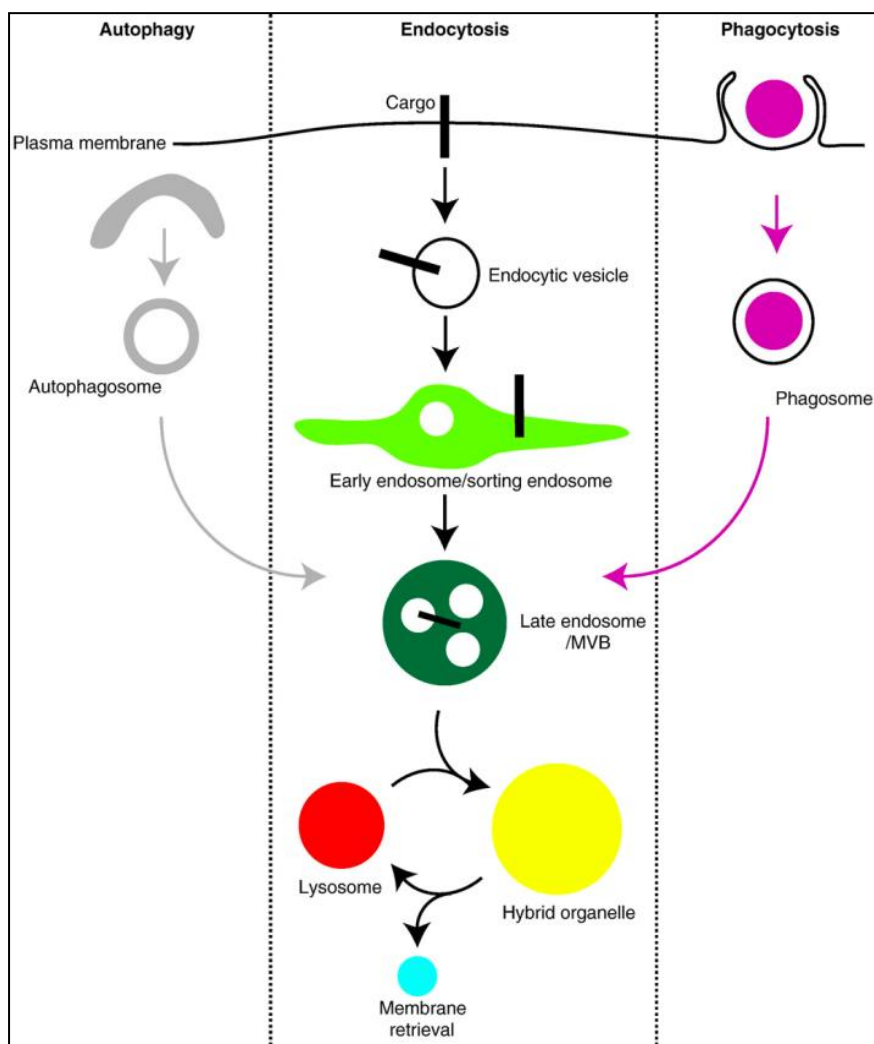


Figure 1. Intracellular pathways to the lysosome. Endocytic cargo is internalized from the plasma membrane and is finally delivered to the lysosomes. In addition, autophagic and phagocytic pathways both feed into the endocytic pathway. Interestingly, Lysosomes are reformed from the hybrid organelle by membrane retrieval (Image reproduced from Pryor *et al* 2009).

1.1.2. Endo-lysosomal pathway

Different processes like autophagy, phagocytosis, exocytosis and endocytosis control the turnover of cargo within the cell and play a pivotal role in maintaining the cell homeostasis. Surprisingly, all these pathways work in concert within the cell in a highly regulated environment. The endocytic pathway is a highly dynamic, regulated and interconnected network of several compartments wherein vesicle fusion and fission occurs. In general, endocytosis refers to the internalization of solutes, macromolecules, fluid, plasma membrane and pathogens (including bacteria, intracellular parasites, and toxins) from the outside environment.

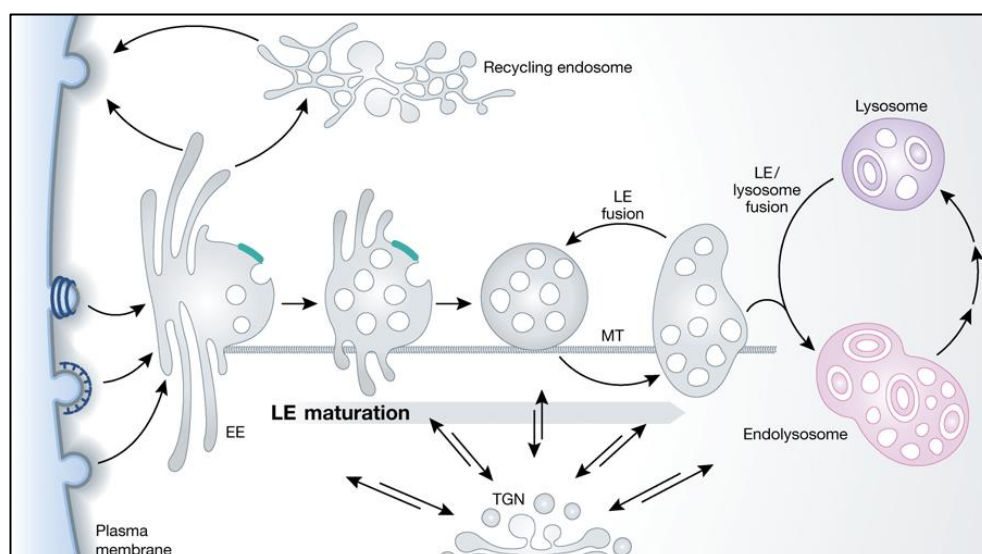


Figure 2. A detailed schematic representation of endo-lysosomal pathway. The internalized cargo is transported to the early endosomes and sorted for recycling through recycling endosomes or degradation to late endosomes. Late endosomes finally fuse with the degradative compartments lysosomes wherein the cargo is degraded to building blocks (Reproduced from Houtari and Helenius 2011).

In endo-lysosomal pathway the internalized primary endocytic vesicle with the cargo is delivered to early endosomes in the peripheral cytoplasm (Houtari and Helenius 2011). Interestingly, at the early endosomes decision is made whether a cargo is recycled back or degraded (Kleine *et al* 2013; Houtari and Helenius 2011). For degradation, cargo traffics through the early endosome mature to late endosomes and is sorted into intraluminal vesicles (ILVs) within the late endosomes (Houtari and Helenius 2011). The fusion of late endosomes with lysosomes forms a hybrid organelle, the endolysosome, in which active degradation takes place (shown in Figure 2).

Endocytosis plays crucial role in many physiological processes like removal of apoptotic bodies, immune surveillance, neurotransmission, termination of signaling by cell surface receptors and, remodeling of the extracellular environment and cell to cell communication (Duncan and Richardson 2012).

Membrane fusion at endosomes, vacuoles and lysosomes involves different regulatory proteins such as coat proteins, small GTPases, soluble NSF attachment protein receptors (SNAREs), and tethering factors. I will further discuss the roles of small GTPases and tethering factor in late endosome-lysosome fusion. Rabs, Arfs and Arf-like small GTPases are members of the Ras superfamily of GTPases, with well-established functions in membrane-trafficking pathways (Burd *et al* 2004). The small GTPases recruit their effectors such as the tethering factors to mediate vesicle fusion. Two homologous tethering complexes called CORVET (Class C core vacuole/endosome transport) and the vacuolar HOPS (homotypic vacuole fusion and protein sorting) functions in the endo-lysosomal pathway (shown in Figure 3). CORVET and HOPS share four of the six subunits, interact with distinct Rab GTPases and SNARE proteins and can tether membranes (Balderhaar *et al* 2013).

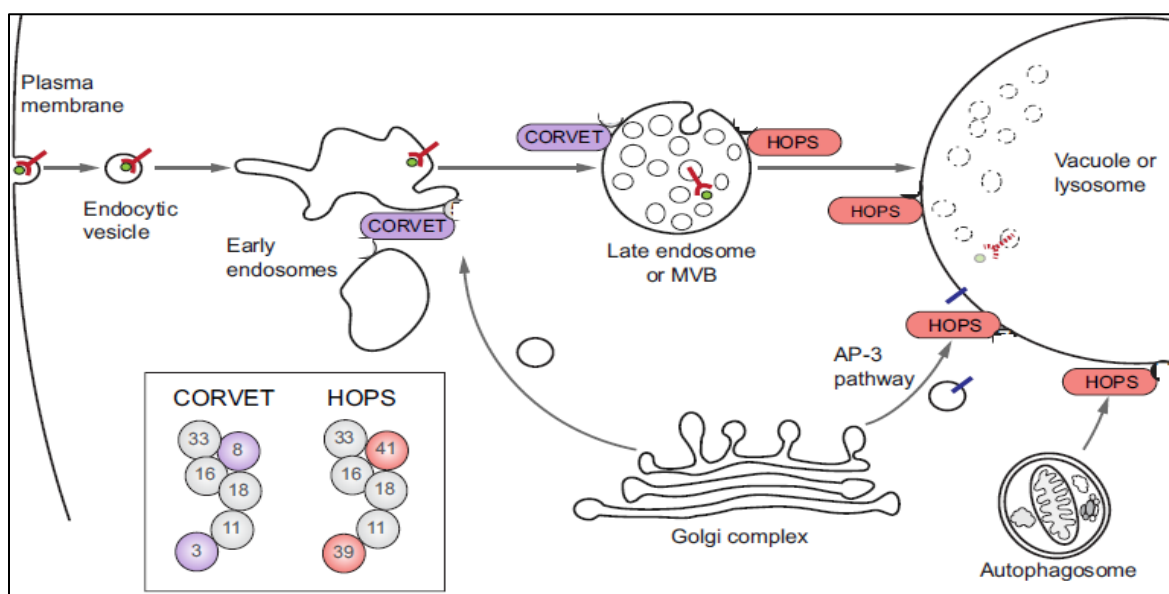


Figure 3. Schematic representation of CORVET and HOPS function within the endo-lysosomal pathway. CORVET functions in endosome-endosome fusion. HOPS complex is required for fusion of late endosome with vacuole/ lysosome, homotypic vacuole–vacuole/ lysosome fusion and for fusion of autophagosomes with the vacuole (Modified from Balderhaar *et al* 2013).

1.1.3. HOPS Complex

HOPS complex is a multi-subunit protein complex discovered in the yeast *Saccharomyces cerevisiae*. Mammalian HOPS assembles into a hexameric complex. The four subunits vacuole protein sorting (Vps) 11, Vps16, Vps18 and Vps33 form the core complex while the two subunits Vps39 and Vps41 are the accessory subunits (shown in Figure 4). In yeast, the knockout of the core subunits results in absence of vacuole while the knockout of accessory subunits results in fragmented vacuole. Recent cryo-EM studies have revealed the shape of the HOPS complex and arrangement of the various Vps subunits within this complex (Bröcker *et al* 2012).

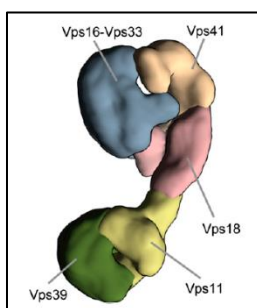


Figure 4. Model of eukaryotic HOPS tethering complex. This model is based on electronic microscopy (EM) combined with single-particle analysis and tomography (Reproduced from Bröcker *et al* 2012).

HOPS complex is known to function in early to late endosome transition and lysosome biogenesis (Solinger and Spang 2013). HOPS subunits regulate trafficking to lysosomes. It acts as a bridge connecting the lysosomes with the late endosome/ autophagosome and mediating their fusion (shown in Figure 5).

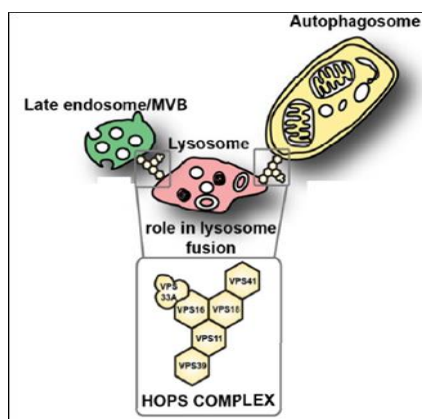


Figure 5. Function of HOPS complex. HOPS complex mediates the fusion of late endosome/ autophagosome with lysosomes by acting like a bridge between the two (Modified from Wartosch *et al* 2015).

1.1.4. HOPS Subunit Vps41

Among all the six subunits of the HOPS complex, Vps41 is the only subunit of HOPS complex that localizes to the lysosomes when expressed in cells by itself (shown in Figure 6). Moreover, Vps41 recruits the rest of the HOPS subunits to the lysosomes by subunit-subunit interaction (Khatter *et al* 2015). This function of Vps41 is conserved from yeast to humans. The small GTPase Arl8b (in humans) or Rab7 (in yeast) interacts with Vps41 and recruit it to the lysosomes/vacuolar membranes (Khatter *et al* 2015). Apart from its role in lysosomal trafficking, Vps41 has been implicated in neuroprotection against α -synuclein protein aggregates (Ruan *et al* 2010). hVps41-mediated neuroprotection against α -synuclein protein aggregates has been extensively studied in *C. elegans* and in mammalian cell culture model systems (Harrington *et al* 2012).

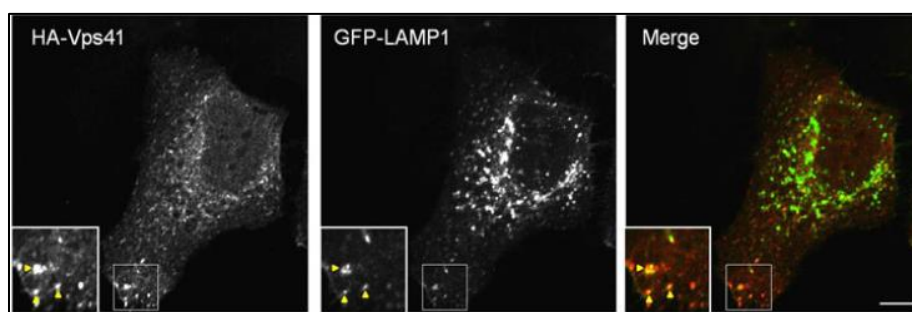


Figure 6. Vps41 subunit of HOPS complex localizes to the lysosomes. Cells overexpressed with HA-Vps41 and GFP-Lamp1 were immunostained against HA tag. HA-Vps41 strongly colocalized with LAMP1 positive lysosomes at the periphery of cell (Reproduced from Khatter *et al* 2015).

The structure of hVps41 is predicted to have four domains namely WD40, tetratricopeptide repeat (TPR)-like domain, clathrin heavy chain repeat (CHCR) and RING-H2 zinc finger domain (shown in Figure 7). Arl8b recruits hVps41 to the lysosomes by interacting with its WD40 domain present at the N terminus (Khatter *et al* 2015).

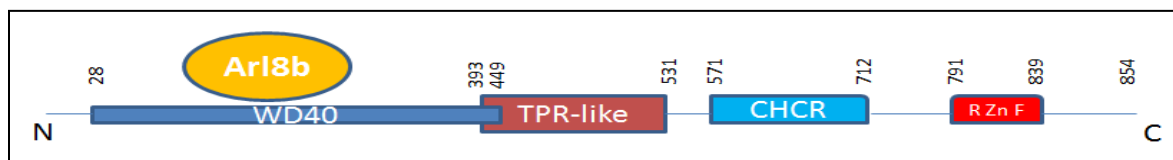


Figure 7. Domain architecture of Vps41 subunit of HOPS complex. hVps41 is predicted to have 4 domains namely WD40, TPR-like domain, CHCR and RING-H2 zinc finger domain.

hVps41 directly interacts with hVps18 subunit of the HOPS complex and further the assembly of HOPS complex takes place on the lysosome in a stepwise manner. In these

experiments, both yeast two-hybrid and co-immunoprecipitation approaches were used to determine their interaction (Khatter *et al* 2015; shown in Figure 8).

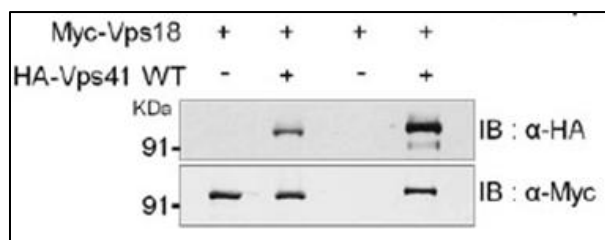


Figure 8. Co-immunoprecipitation of Vps18 by Vps41. HEK293T cells were co-transfected with HA-tagged Vps41 and Myc-tagged Vps18. Vps18 was pulled down by Vps41 (Reproduced from Khatter *et al* 2015).

1.1.5. RING Domains

Really Interesting New Gene (RING) domains are a type of zinc finger domains that bind zinc atoms. RING domains are characterized by a pattern of cysteine and histidine residues that form the zinc coordinating sites. The consensus sequence of RING domains bind two Zn^{2+} atoms in a unique “cross-brace” structure (Rieder *et al* 1997; shown in Figure 9). RING domains are known to perform important functions such as

- protein-protein interaction
- E3 Ubiquitin ligase activity

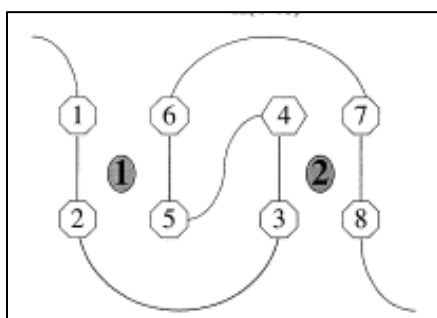


Figure 9. Representation of Zinc metal binding in RING domain. The numbers from 1 to 8 are the cysteine/histidine residues arranged in a pattern so as to incorporate zinc atoms (bold 1 and 2) within zinc metal binding site (Modified from Borden 2000).

The zinc binding activity of RING domains contributes to the diverse functions elicited by these protein domains. Zinc ligation is critical for folding of the domain and for subsequent biological action(s) (Borden 2000). Many proteins such as the promyelocytic leukemia proto-oncogene PML, V(D)J recombination-activating protein (RAG1) and breast and ovarian

cancer tumor suppressor protein, BRCA1, possess a Zn²⁺ binding RING finger motif that is important for the cellular function of these proteins (Brzovic *et al* 1998)

Interestingly, HOPS subunits Vps11, Vps18, Vps41 contain C terminal RING-H2 motifs (Kaur and Subramanian 2015). A previous study on Vps8p, which is part of the CORVET complex, has shown that deletion of its RING motif at its C terminus partially compromises its function (Horazdovsky *et al* 1996). Another study has shown that hVps18 exhibits E3 ubiquitin ligase activity and is capable of regulating adaptor proteins like GGAs (Golgi-localizing, c-adaptin ear domain homology, ADP-ribosylation factor (ARF)-binding proteins) and serum-inducible kinase (SNK) that regulates cell division (Yogosawa *et al* 2006; Yogosawa *et al* 2005)

Domain deletion studies have shown that RING motifs of yeast HOPS subunits Vps18, Vps11 and Vps39 are not needed for HOPS assembly, but functions to regulate the fusion at vacuole (R. L. Plemel *et al* 2011). Recently, contradictory evidence has suggested that interactions between different subunits of mammalian HOPS complex occurs via their RING-H2 motifs, thus the RING-H2 motifs are crucial for assembly of the HOPS complex (Van Der Kant *et al* 2015). In comparison to yeast Vps41p, the metazoan homologue Vps41 has a C terminal RING-H2 motif (Ward *et al* 2001) as depicted in the domain architecture model (shown in Figure 7). It is possible that from yeast to humans the RING domain of Vps41 has evolved for specific function in multicellular organisms. hVps41 RING Zinc finger domain is of C3H2C3-type (C stands for Cysteine and H stands for Histidine) and it spans from 791 AA to 839 AA.

Based on this background knowledge, the main objectives of my thesis were:

- Identification of Vps41 domain essential for its interaction with Vps18 and the critical residues within this domain.
- Identification of Vps18 domain that is essential for its interaction with other HOPS (especially Vps41) subunits and the critical residues within this domain.
- Purification of HOPS subunits Vps39 and Vps18 to characterize the expression of HOPS subunits by synthesis of antibodies against Vps39 and Vps18

1.2 Materials and Methods

1.2.1. Plasmids

HA-tagged Vps41 was gifted by Wade Harper lab (USA). Full length human HOPS complex subunits hVps41 and hVps39 cloned in mammalian expression vector were obtained from C.Liang lab (USA). Vps39 and Vps18 in pMALC2x were previously cloned in the lab. Vps41 C814S H816R and Vps18 in pGADT7 were previously cloned in the lab. HOPS complex subunits such as Vps11, Vps16, Vps33a, Vps39 and Vps41 in pGBKT7 were also previously cloned in the lab. The details of other cloning are shown in detail in Table 1.

1.2.2. Antibodies

Mouse monoclonal antibody against Myc epitope tag was procured from Santa Cruz Biotech. Rabbit polyclonal antibody against HA epitope tag was obtained from Sigma and Mouse monoclonal antibody against HA epitope tag was obtained from Covance. Rabbit polyclonal antibody against Vps33a and Vps11 was obtained from ProteinTech. Mouse monoclonal antibody against human LAMP1 was obtained from BD transduction laboratory. Goat anti-mouse-IgG and anti-rabbit-IgG HRP-conjugated antibodies were obtained from Jackson ImmunoResearch Laboratories. Alexa-Fluor-conjugated secondary goat anti-mouse-IgG and goat anti-rabbit-IgG antibodies 488, 568, 647 were purchased from Invitrogen.

1.2.3. Cell Culture and Transfection

HeLa and Human Embryonic Kidney (HEK) 293T cell lines were grown and maintained in Dulbecco's Modified Eagle medium (DMEM; Life Technologies) supplemented with 10% FBS (Life Technologies) at 37⁰C in CO₂ incubator. The media of the cell lines were changed occasionally and cell splitting was done based on confluency. For pulldown experiments like co-immunoprecipitation and GST pulldown, HEK293T cells in a 60mm dish were transfected using transfection reagents including Lipofectamine or Fugene as per the manufacturer's instruction. For colocalization studies, HeLa cells were grown on coverslips for one day and transfected with desired plasmids.

1.2.4. Immunostaining

HeLa cells were plated on glass coverslips and transfected with different combinations of plasmid DNA. Post 16 to 20 hours of transfection, cells were fixed with 4% of PFA in PHEM (60mM PIPES, 10mM EGTA, 25mM HEPES, 2mM MgCl₂) buffer for 10 minutes and washed with 1X PBS thrice. Further, blocking of non-specific staining was done with PHEM buffer containing 5% FBS and 0.2% Saponin for an hour. After blocking, the cells were incubated with primary antibody in PHEM buffer for 1 hour followed by three times wash with 1X PBS. Cells were then incubated with secondary antibodies conjugated with Alexa fluorophores in PHEM buffer for 30 minutes. After three washes with 1X PBS, the cells were mounted with fluoromount G (Southern Biotech) and were analyzed using confocal microscopy.

1.2.5. Imaging using Confocal Microscopy

Zeiss Laser Scanning Microscope (LSM) 710 confocal microscope was used for the imaging of immunostained coverslips. All images were captured using 60X oil immersion objectives. Optical parameters were set at the beginning and kept constant throughout the imaging of a single coverslip. Excitation and emission wavelength of Alexa 488 (green channel), Alexa 568 (red channel) and Alexa 647 (blue channel) fluorophores were adjusted with the help of filters. The images were edited using Photoshop and ImageJ Launcher.

1.2.6. Site-directed Mutagenesis

Stratagene's QuikChange™ site-directed mutagenesis kit was used as per the manufacturer's instructions for incorporating site-specific mutation in the double-stranded plasmids. The sequence of the SDM primers for the constructs are as follows: hVps41 C791S C794S (FP:5'GATGAGGAGAACATCAGTGAGTCGAGCCTTCCCCTATTC3',RP:5'GAATAGGGGAAAGGCTCGACTCACTGATGTTCTCCTCATC3'), hVps41 H819R C822S (FP:5'GCCGCGCATGTTCCGCAAGGAGAGCCTGCCCATGCC3',RP:5'GGGCATGGCAGGCTCTCCTTGC GGAACATGCGCCGGC3'), hVps18 C853S C856S (FP:5'GAGCCCCAGGACAAAAGTGCCACCAGCGACTTCCCCCTGC3',RP:5'GCAGG

GGGAAGTCGCTGGTGGCACTTTTGTCTGGGGCTC3'), hVps18 C870S H872R (FP:5'CTTTTACCTCTTCCTCAGTGGCCGTATGTTCCATGCTGA,RP:5'TCAGCATG GAACATACGGCCACTGAGGAAGAGGTAAAAAG3')

1.2.7. Yeast two hybrid

Proteins to be fused with activation domain were cloned in pGADT7 vector and the other proteins were cloned in pGBKT7 vector. *S. cerevisiae* strain AH109 or Y2H Gold was transformed with the prey and bait (0.5µg each) and the co-transformants were confirmed on -2 plate (-Leu-Trp+His) at 30⁰C. Further, after 3 days the yeast was spotted on selective media like -3 plate (-Leu-Trp-His) on which yeast grows if and only if an interaction between the prey and bait happens. In some reactions, a more stringent selective media like 3-AT plate was used, which is a competitive inhibitor of Histidine.

1.2.8. Co-immunoprecipitation

In this thesis work, co-immunoprecipitation was done to check the interaction of Myc-tagged Vps18 with different mutants of HA-tagged Vps41 and *vice versa*. HEK293T cells were co-transfected with the respective plasmids using the transfection reagent Lipofectamine. After 12-16 hours of transfection, the cells were collected and lysed in ice-cold lysis buffer (20 mM Tris-HCl pH 7.4, 150 mM NaCl, 1 mM EDTA, 0.5% NP-40, 1 mM sodium orthovanadate) with protease inhibitor cocktail and PMSF for 20 minutes at 4⁰C under tumbling. After lysis, the cell debris was separated from the supernatant by high-speed centrifugation (14,000 rpm at 4⁰C). The appropriate beads were washed thrice with the lysis buffer and incubated with the cell lysates tumbling at 4⁰C for 3 hours. The beads were washed with the lysis buffer. The bound proteins were eluted from the beads by boiling with 4X sample buffer at 99⁰C. The input samples and the co-immunoprecipitation samples were run on 8% or 10% SDS PAGE gel.

1.2.9. Western blotting

After running SDS PAGE, the gel was transferred onto a nitrocellulose membrane in transfer buffer for one and half hour. The blot was blocked in 10% skim milk for an hour. After

blocking, the blot was washed with PBST (PBS, 0.03% Tween 20) and incubated with the primary antibody in PBST for 1 hour. The blot was washed with PBST for three times and incubated with secondary antibody for 30 minutes. After three washes with PBST, enhanced chemiluminescence substrate reaction was performed and the signal was obtained on the X-ray film.

1.2.10. GST pulldown

GST and GST–Arl8b were purified using standard methods, and GST pulldown assays and was performed similar to the protocol of Methods and Materials Section 8.

1.2.11. Protein purification

MBP-Vps39 or MBP-Vps18 plasmids were transformed in BL21 strain of *Escherichia Coli*. A primary culture was set up in LB with antibiotic and the transformed colony. After 24 h, a secondary culture with 1% inoculum from the primary culture was prepared in a larger volume of LB. The culture was incubated at 37⁰C under shaking (200rpm) for 1.5 to 2 hours until the O.D is in the range of 0.4 to 0.6. The culture was induced with 0.5mM IPTG for 5 hours at 30⁰C under shaking (200rpm). The culture pellet was resuspended in appropriate amount of column buffer (20mM Tris-Cl pH 7.4, 200mM NaCl, 1mM EDTA, 10mM β -mercaptoethanol) and Protease Inhibitor tablet and sonicated to lyse open the cells. The supernatant and the pellet were separated out with high speed centrifugation. The supernatant was bound with washed amylose beads for 3 hours at 4⁰C under tumbling. After 3 hours, the beads were washed off from unbound and non-specific proteins with column buffer. The proteins were eluted from the amylose beads using 0.4M Maltose for overnight, 2 hours or 1 hour. SDS PAGE gel was run to confirm the induction of protein and the eluates in appropriate amount. The eluted protein was then loaded in AKTA machine which was set at the correct parameters according to the size of the protein that was to be purified. The post-AKTA fractions were stored at 4⁰C and finally concentrated into a final solution by buffer exchange method. The concentration of the protein was estimated using the spectrophotometer and the calculation using Beer-Lambert's law.

1.2.12. Antibody purification test

The purified proteins were sent to the company for synthesizing antibodies against them by injecting into Rabbit. After this immunization process, the collected serum with raised antibodies was sent back to us. Primarily, the antibody was tested to detect the expression of endogenous Vps39 and Vps18 in HeLa and HEK293T cell lines with 1:500 dilution. HeLa and HEK293T cell lysates were created using ice-cold lysis buffer (25 mM Tris-HCl pH 7.4, 150 mM NaCl, 1 mM EDTA, 1% Triton X-100 and protease inhibitor cocktail).

To purify antibody against MBP-Vps39 protein from the serum, Protein G coated beads were used. The protein G slurry was washed thrice with binding buffer. The washed G slurry was incubated with 2 ml serum against MBP-Vps39 for 2 hour at 4⁰C. After binding, the supernatant was collected and the beads were washed with large volumes of wash buffer. The bound proteins were eluted from the beads with glycine buffer in different fractions. The eluate was neutralized with Tris-Cl neutralization buffer. The concentration of the eluates was checked using the spectrophotometer. A SDS PAGE was run with HeLa lysate, HA-Vps39 overexpressed HEK293T lysate, MBP-Vps39 (10µg) protein and MBP-Vps18 (10µg) protein. The gel was transferred onto a blot and incubated with first two eluates (Fraction 1 and Fraction 2).

Purified protein was also used to purify the antibody out of the solution. 10µg protein was incubated with 2 ml serum against MBP-Vps39 for 2 hour at 4⁰C. After incubation, prewashed amylose resin was bound with the above mixture for 45 minutes at 4⁰C. After binding, the resin was washed off large volumes of column buffer. The bound proteins were eluted from the beads with glycine buffer in different fractions. The eluate was neutralized with Tris-Cl neutralization buffer. A SDS PAGE was run with HeLa lysate, HA-Vps39 overexpressed HEK293T lysate, control knockdown and Vps39 knockdown samples. The gel was transferred onto a blot and incubated with first two eluates (Fraction 1 and Fraction 2). As a more stringent condition, the primary antibody was incubated in 10% skim milk overnight and the blot was washed with high salt buffer (500Mm NaCl, 0.2%SDS in 1X PBS) for 15-30s before developing.

2. SUMMARY AND CONCLUSIONS

2.1 Results and Discussion

2.2 Future Prospects

2.1 Results and Discussions

From invertebrates to vertebrates, HOPS complex is known to function in mediating the fusion of late endosomes with the lysosomes. Our lab has previously shown that the small GTPase Arl8b interacts with the Vps41 subunit of HOPS complex thereby recruits it to the lysosomal membrane (Khatter *et al* 2015). Vps41 leads to the assembly of other HOPS subunits on the lysosomes in a hierarchical manner. The N-terminal WD40 domain of Vps41 binds to Arl8b and the C terminus interacts with Vps18 subunit of HOPS complex (Khatter *et al* 2015; shown in Figure 10).

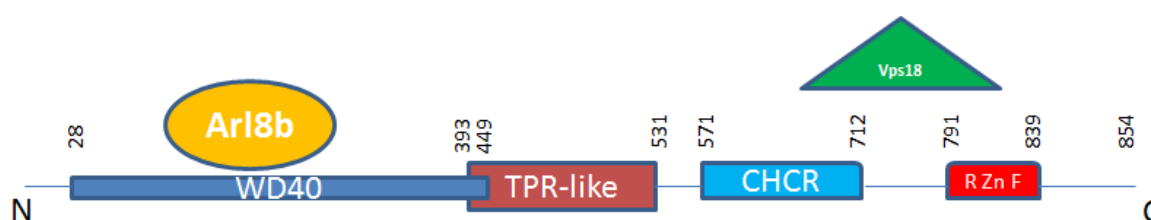


Figure 10. Domain architecture of Vps41 depicting interactions with different partners. Arl8b binds to the N-terminal WD40 domain of Vps41 whereas Vps18 interacts with C-terminus of Vps41.

The direct interaction between Vps41 and Vps18 is supported by results of co-immunoprecipitation and yeast two hybrid analysis (shown in Figure 11). In this study we have investigated the domain of Vps41 on the C terminal that is essential for its interaction with Vps18. Further, we have pinned down the amino acid residues within the domain that are involved in the interaction with Vps18 using co-immunoprecipitation and colocalization studies.

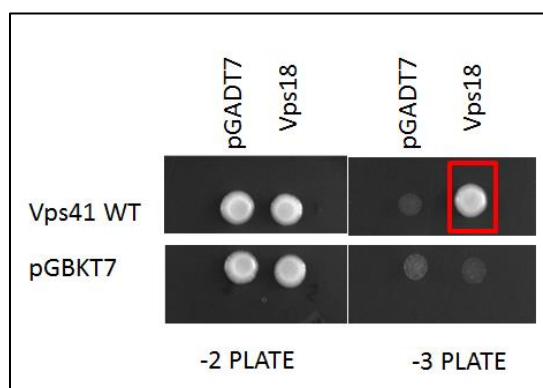


Figure 11. Yeast two hybrid interaction of Vps41 (cloned in binding domain vector) **with Vps18** (cloned in activation domain vector) was tested using pGBKT7/pGADT7 system. Yeast were plated on non-selective media (+His) to confirm viability and on selective media (-His) to detect interaction. A distinct spot corresponding to Vps41-Vps18 interaction was seen.

2.1.1. The Ring Domain of Vps41 Is Essential for Its Interaction with Vps18

To find out the domain involved in the interaction between Vps41 and Vps18, we created certain domain deletion mutants that lack C terminal domains within Vps41. Further, co-immunoprecipitation was done to analyze the interaction. The expression of these domain mutants was confirmed by confocal microscopy.

A. hVps41-713X does not interact with hVps18

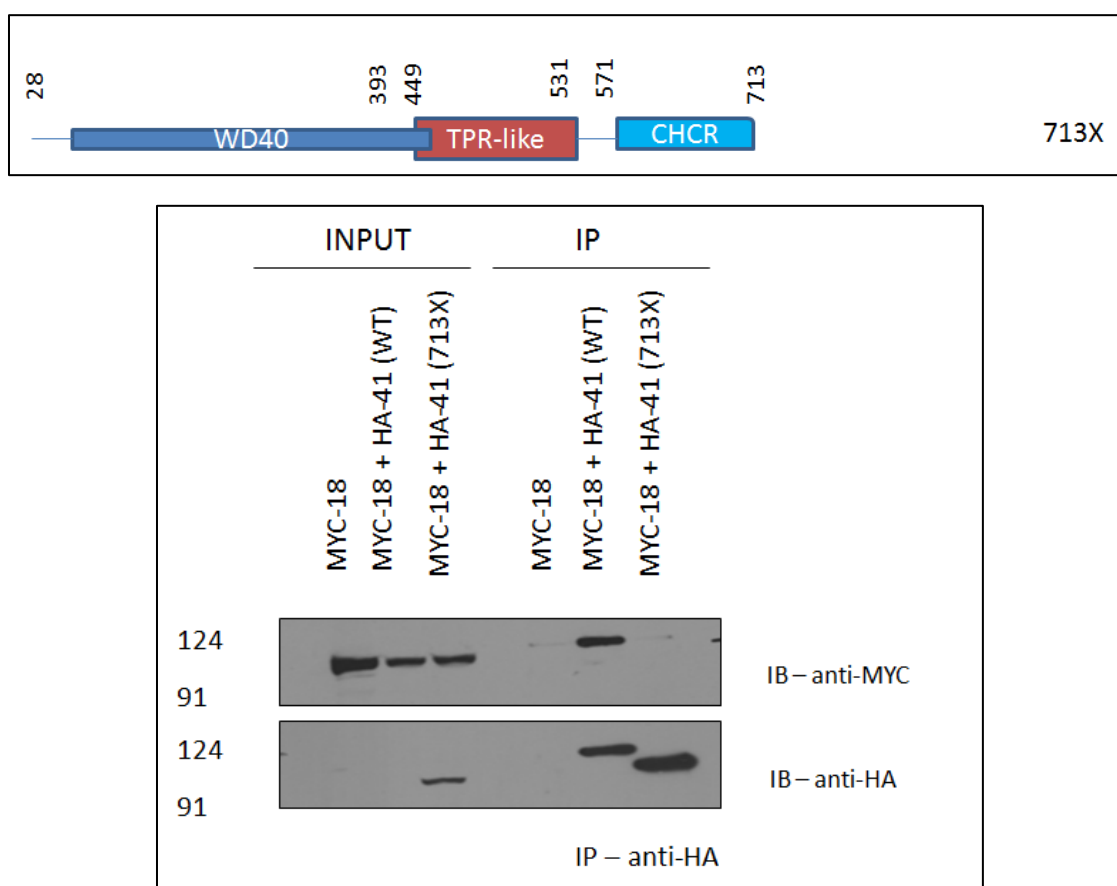


Figure 12. Domain architecture of Vps41 713X mutant and Co-immunoprecipitation analysis of Vps41 713X with Vps18. HEK293T cells were co-transfected with HA-Vps41 713X and Myc-Vps18. Vps18 was not pulled down by Vps41 713X compared to Vps41 WT.

To start with, we used the domain deletion mutant Vps41 713X that lack C-terminal domains after CHCR domain. HEK293T cells were co-transfected with HA-tagged Vps41 713X subunit and Myc-tagged Vps18 subunit of HOPS complex. HEK293T cells were also transfected with Myc-tagged Vps18 as a negative control and co-transfected with wild type

HA-tagged Vps41 subunit and Myc-tagged Vps18 as a positive control. Co-immunoprecipitation was done according to the standard protocol described in the methods section. The fractions were collected and loaded on 8% SDS gel. Later the expression and immunoprecipitation of the constructs were analyzed by western blot by probing the blot against anti-Myc and anti-HA. Vps41 WT-dependent immunoprecipitation of Vps18 was observed as expected. However the domain deletion mutant HA-tagged Vps41 713X did not bind Myc-tagged Vps18 supported by the absence of band on the blot (shown in Figure 12).

A previous study from our laboratory has shown that hVps18 is recruited by its direct interaction with hVps41 to LAMP1-positive lysosomes (Khatter *et al* 2015) (shown in Figure 13). Since we found that Vps41 713X does not bind to Vps18, we tested whether this mutant of Vps41 recruits hVps18 to the LAMP1-positive lysosomes. Confocal analysis revealed that HA-tagged Vps41 713X localized to the LAMP1-positive lysosomes, however, the localization of Vps18 to lysosomes was lost upon overexpression of HA-tagged Vps41 713X (shown in Figure 13).

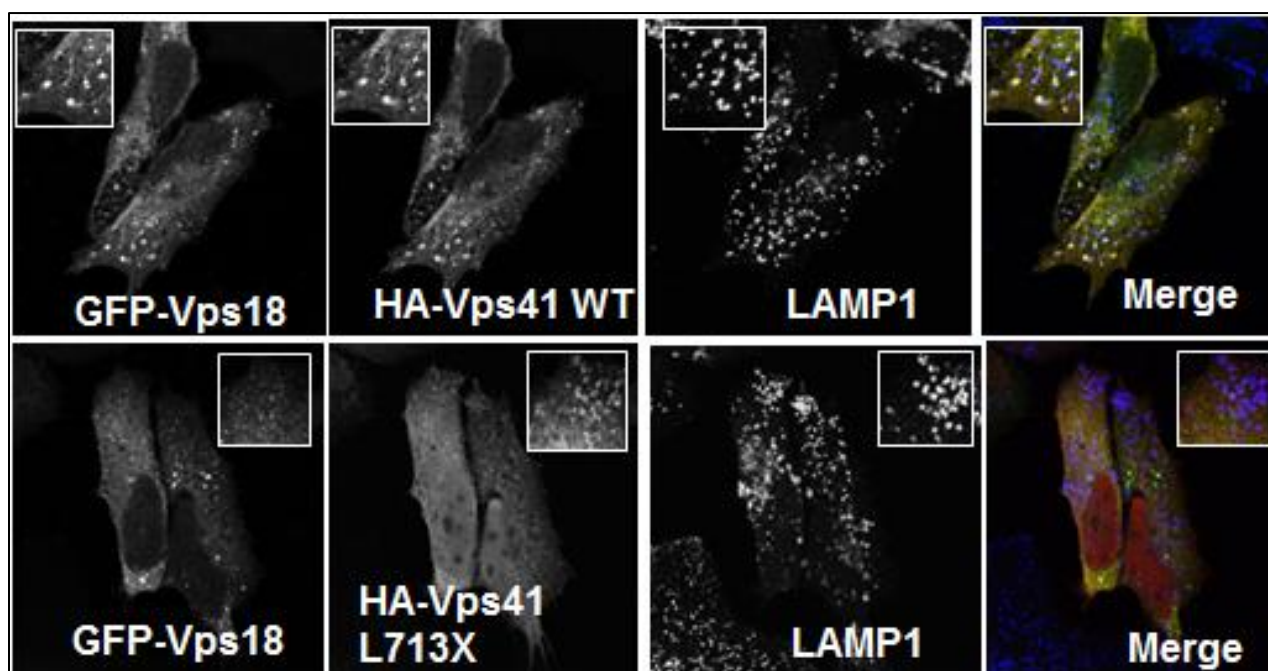


Figure 13. Colocalization study of Vps41 713X domain deletion mutant with Vps18. HeLa cells were co-transfected with GFP-tagged Vps18, and HA-tagged Vps41 in one set and with GFP-tagged Vps18, HA-tagged Vps41 L713X in another set. Colocalization was analyzed including the endogenous LAMP1 expression by confocal microscopy. HA-Vps41 L713X failed to recruit GFP-Vps18 onto the lysosomes.

B. hVps41-791X does not interact with hVps18

Next, we created domain deletion mutant of Vps41 lacking the RING finger motif and the C-terminal tail (Vps41 791X) and tested its interaction with Vps18 using co-immunoprecipitation assay. To this end, HEK293T cells were co-transfected with HA-tagged Vps41 791X subunit and Myc-tagged Vps18 subunit of HOPS complex. HEK293T cells were also transfected with Myc-tagged Vps18 as a negative control and co-transfected with HA-tagged Vps41 subunit and Myc-tagged Vps18 as a positive control. Vps41 WT-dependent pulldown of Vps18 was observed as expected. However the domain deletion mutant HA-tagged Vps41 791X did not bind Myc-tagged Vps18 supported by the absence of band on the blot (shown in Figure 14).

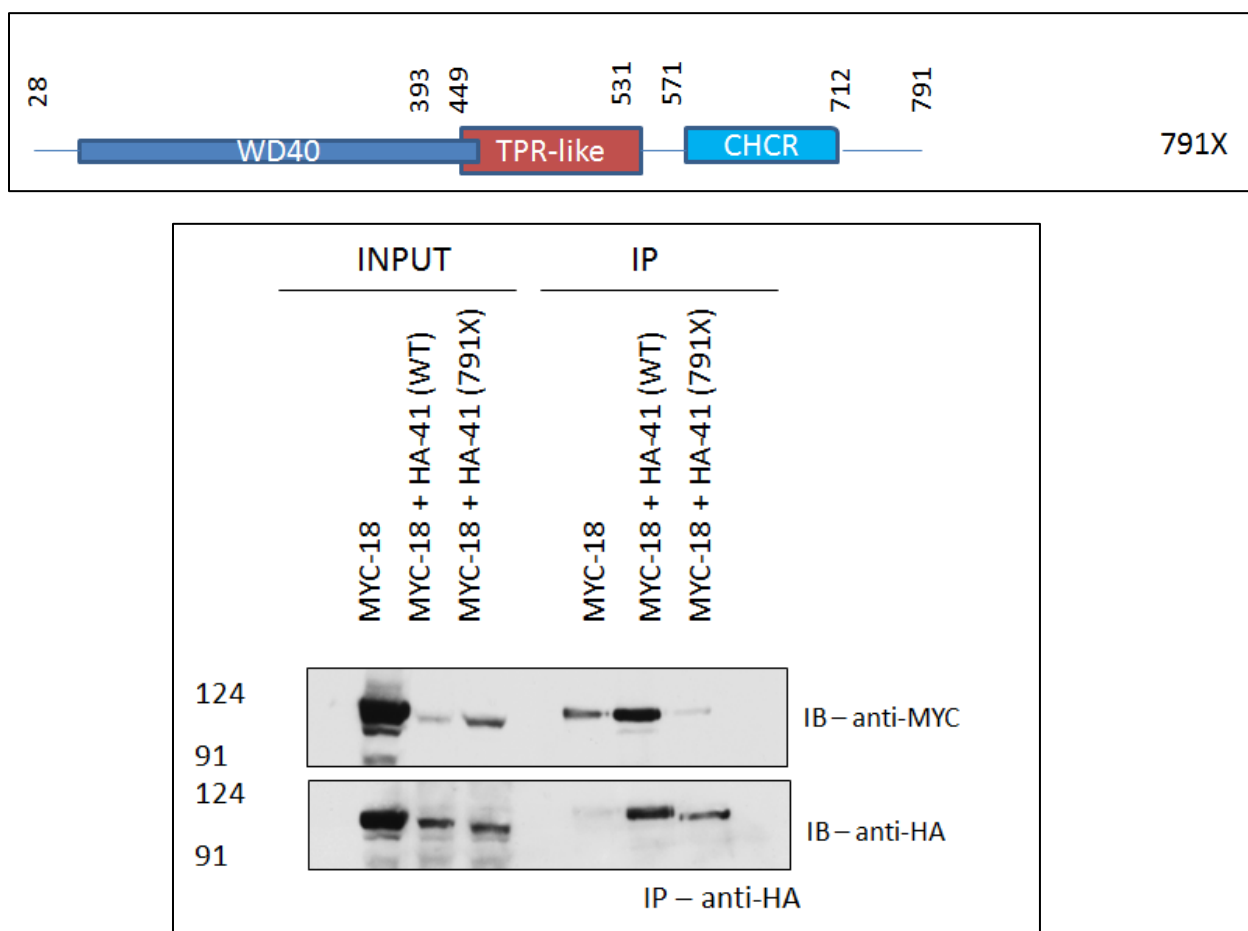


Figure 14. Domain architecture of Vps41 791X mutant and Co-immunoprecipitation analysis of Vps41 791X with Vps18. HEK293T cells were co-transfected with HA-Vps41 791X and Myc-Vps18. Vps18 was not pulled down by Vps41 791X compared to Vps41 WT.

C. hVps41-WT and hVps41-839X interacts with hVps18

Further, to identify the minimal domain of Vps41 that interacts with Vps18, we created Vps41 839X domain deletion mutant that lacks only the C-terminal tail. Interestingly, the domain deletion mutant HA-tagged Vps41 839X immunoprecipitated Myc-tagged Vps18 similar to Vps41 WT indicated by the band on the blot (shown in Figure 15).

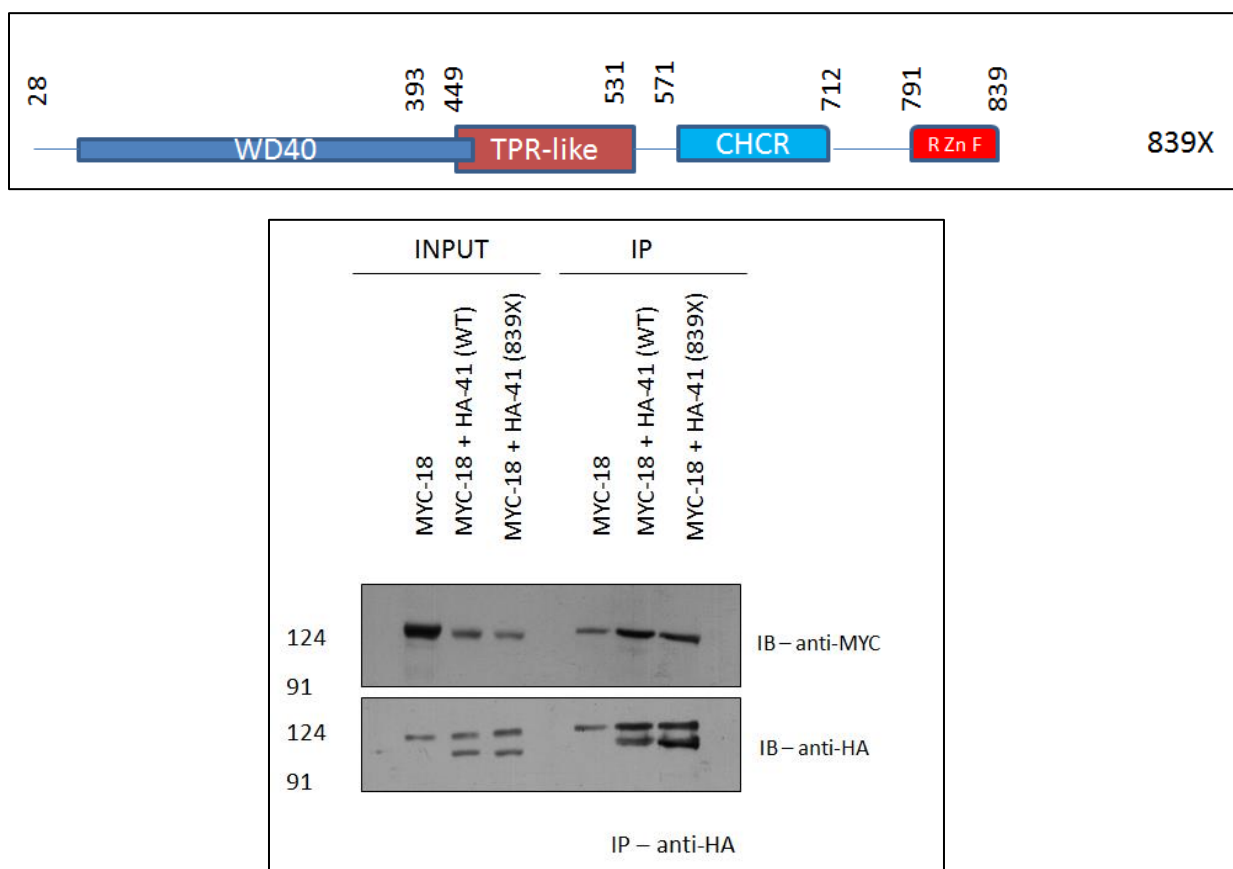


Figure 15. Domain architecture of Vps41 839X mutant and Co-immunoprecipitation analysis of Vps41 839X with Vps18. HEK293T cells were co-transfected with HA-Vps41 839X and Myc-Vps18. Vps18 was pulled down by Vps41 839X similar to Vps41 WT.

2.1.2. The cysteine and histidine residues of hVps41 RING domain are critical for its interaction with hVps18

The cysteine and histidine residues in the RING domains mediate the Zinc coordination. Zinc coordination in RING domain containing proteins is important for the elicitation of their

functions. Hence we investigated the involvement of the cysteine and histidine residues in hVps41 RING domain in the interaction process with hVps18.

The Vps41 RING-H2 domain consists of 8 cysteine and histidine residues in total forming two Zinc coordinating sites (shown in Figure 16). We mutated these residues in HA-tagged Vps41 construct in a sequential manner using site directed mutagenesis to elucidate if the zinc coordination residues are required for interaction with Vps18. The cysteine residues were mutated to serine residues and histidine residues were mutated to arginine residues. These substitutions that match closely the size and charge of the cysteine and histidine residues do not disrupt the folding of the RING-H2 domain but disrupt its zinc coordination function.

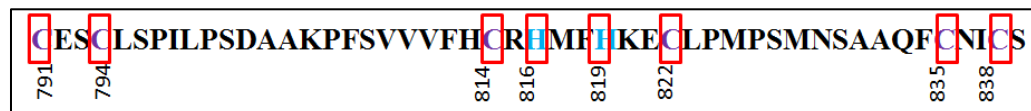


Figure 16. Vps41 RING-H2 domain. The highlighted residues are the cysteine residues and histidine residues within the RING-H2 domain of Vps41 that spans from 791AA to 839AA.

A. hVps41 Δ RING does not interact with hVps18

The hVps41 Δ RING mutant has the first six cysteine or histidine residues mutated to serine and arginine residues (C791S C794S C814S H816R H819R C822S) respectively. HEK293T cells were co-transfected with HA-tagged Vps41 Δ RING and Myc-tagged Vps18 subunit of HOPS complex. HEK293T cells were also transfected with Myc-tagged Vps18 as a negative control and co-transfected with WT HA-tagged Vps41 and Myc-tagged Vps18 as a positive control. Unlike the wild type Vps41, HA-tagged Vps41 Δ RING did not bind Myc-tagged Vps18 supported by the absence of band on the blot (shown in Figure 17). HA-tagged Vps41 Δ RING also failed to recruit other HOPS complex subunits such as Vps33a in comparison to Vps41 WT. This strengthens the fact that the interaction of Vps41 with Vps18 is an essential step for the recruitment of other HOPS subunits onto the lysosomes and the complete assembly of the HOPS complex.

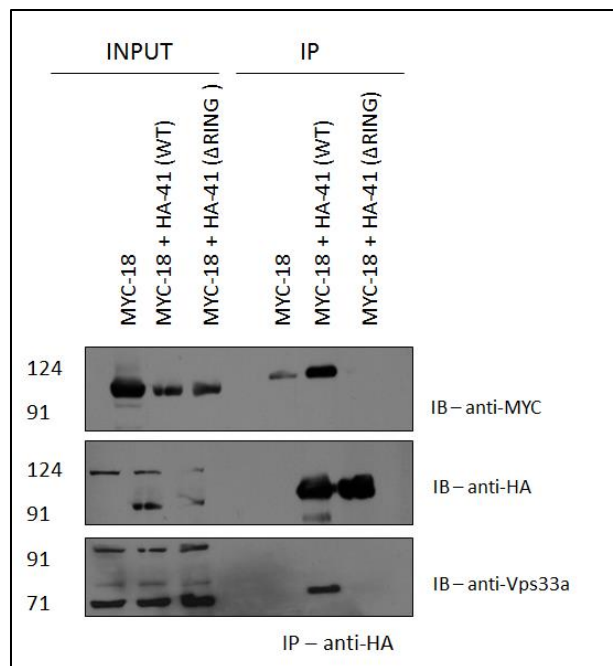


Figure 17. Co-immunoprecipitation of Vps41 Δ RING (First 6 Cysteines/ Histidines are mutated) with Vps18. HEK293T cells were co-transfected with HA-Vps41 Δ RING and Myc-Vps18. Vps18 was not pulled down by Vps41 Δ RING compared to Vps41 WT. Further, pulldown of other HOPS subunit like Vps33a was not observed in Vps41 Δ RING compared to Vps41 WT.

B. hVps41 Δ C3H does not interact with hVps18

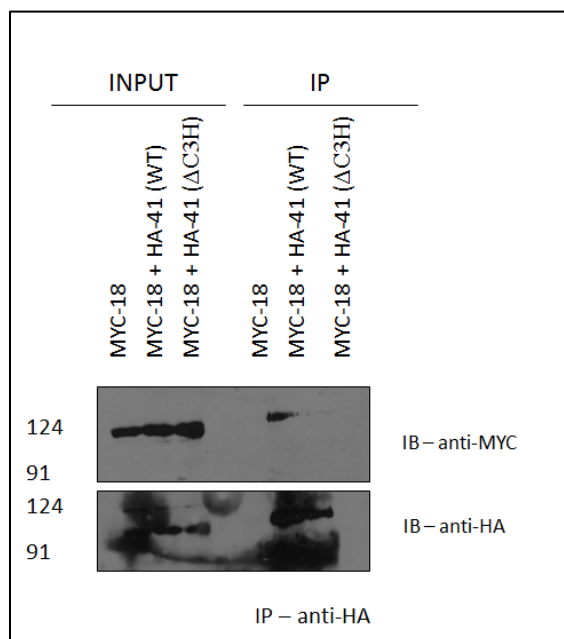


Figure 18. Co-immunoprecipitation of Vps41 Δ C3H (First 4 Cysteines/ Histidines are mutated) with Vps18. HEK293T cells were co-transfected with HA-Vps41 Δ C3H and Myc-Vps18. Vps18 was not pulled down by Vps41 Δ C3H compared to Vps41 WT.

Next, we created a mutant Δ C3H (C791S C794S C814S H816R) mutant that has the first 4 cysteine or histidine residues mutated to serine and arginine residues respectively. Co-immunoprecipitation analysis showed Vps41-WT dependent precipitation of Vps18 as expected. Whereas, the mutant HA-tagged Vps41 Δ C3H did not bind Myc-tagged Vps18 (shown in Figure 18).

C. hVps41 C791S C794S does not interact with hVps18

Based on our previous results and to narrow down the crucial residues in Vps41 RING that are essential for its interaction with Vps18, we created HA-tagged hVps41 C791S C794S that has only substitution of two residues. C791 and C794 are part of the first zinc coordinating site. First Zinc coordinating sites are more important than the second Zinc coordinating sites in terms of the function of the RING domains (Borden 2000). Co-immunoprecipitation experiment showed Vps41 WT-dependent precipitation of Vps18 as expected. However the mutant HA-tagged Vps41 C791S C794S did not bind Myc-tagged Vps18 similar to the Vps41 mutants lacking RING-H2 domain (shown in Figure 19).

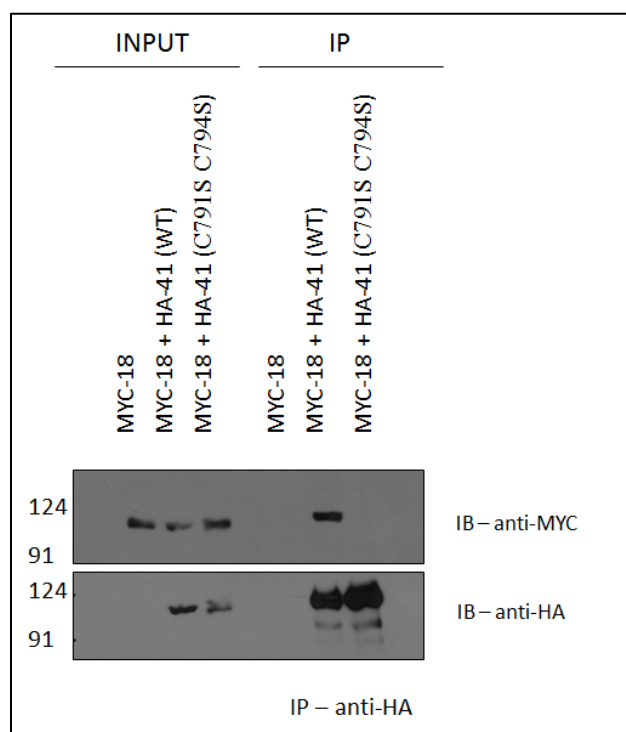


Figure 19. Co-immunoprecipitation of Vps41 C791S C794S (First 2 Cysteines are mutated to Serines) with Vps18. HEK293T cells were co-transfected with HA-Vps41 C791S C794S and Myc-Vps18. Myc-Vps18 only is a negative control whereas HA-Vps41 WT and Myc-Vps18 is a positive control. The mutant Vps41 C791S C794S did not pull down Vps18 as compared to Vps41 WT.

Further we performed yeast two-hybrid analysis to confirm the conclusion that the C791S C794S mutant of Vps41 does not interact with Vps18. To test this, Vps41 WT and Vps41 C791S C794S were cloned in fusion with Gal4 binding domain and were used as the bait. Vps18 was cloned in fusion with Gal4 activation domain. After transformation, yeasts were plated on -2 plate (-Leu -Trp +His) for the confirmation of cotransformants and on -3 plate (-Leu -Trp -His) to detect direct interaction. Even after 3 to 4 days of incubation, no interaction between Vps41 C791S C794S and Vps18 subunits of HOPS complex was observed, whereas strong growth of yeast was observed with Vps41 WT (shown in Figure 20).

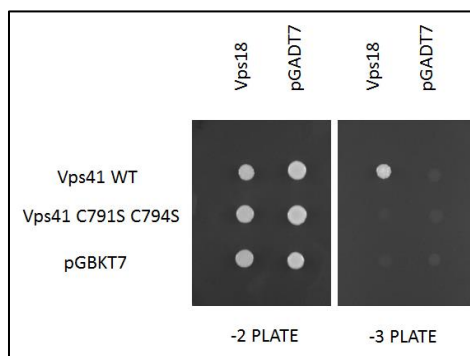


Figure 20. Yeast two hybrid interactions of Vps41 and Vps41 C791S C794S (cloned in binding domain vector) with Vps18 (cloned in activation domain vector). A distinct spot for interaction between Vps41 WT and Vps18 was observed. The RING mutant Vps41 C791S C794S did not interact with Vps18.

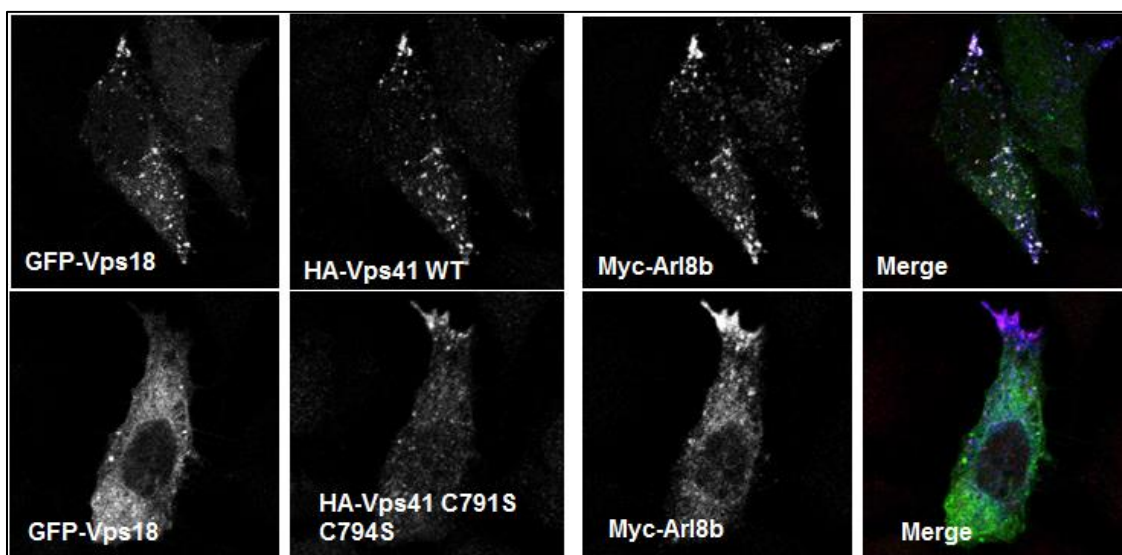


Figure 21. Colocalization study of Vps41 C791S C794S mutant with Vps18. HeLa cells were co-transfected with GFP-tagged Vps18, Myc-tagged Arl8b and HA-tagged Vps41 in one set and with GFP-tagged Vps18, Myc-tagged Arl8b and

HA-tagged Vps41 C791S C794S in another set. Colocalization was analyzed by confocal microscopy. Compared to HA-Vps41 WT, HA-Vps41 C791S C794S failed to recruit Vps18 onto Myc-Arl8b positive lysosomes.

To study the localization of Vps41 C791S C794S, HA-tagged Vps41 C791S C794S with GFP-tagged Vps18 and Myc-tagged Arl8b were over expressed in HeLa cells. The cells were immunostained with antibodies against HA tag and Myc tag. Confocal analysis revealed that HA-tagged Vps41 C791S C794S failed to colocalize with GFP-tagged Vps18 on the lysosomes (shown in Figure 21).

Moreover, GST pulldown experiment was done to check the interaction of Vps41 WT and Vps41 C791S C794S with Arl8b, as binding to Arl8b determines the lysosomal localization of Vps41. HEK293T cells were overexpressed with HA-tagged Vps41 and HA-tagged Vps41 C791S C794S separately. The cell lysates were then incubated with GST only beads and GST-Arl8b beads. GST pulldown was done according to the standard protocol described in the methods section. The fractions were collected and loaded on 8% SDS gel. Later the expression of the HA-tagged Vps41 and HA-tagged Vps41 C791S C794S were analyzed by western blot by probing the blot against anti-HA. HA-tagged Vps41 and HA-tagged Vps41 C791S C794S were pulled down by the GST-Arl8b coated beads in a similar fashion (shown in Figure 22).

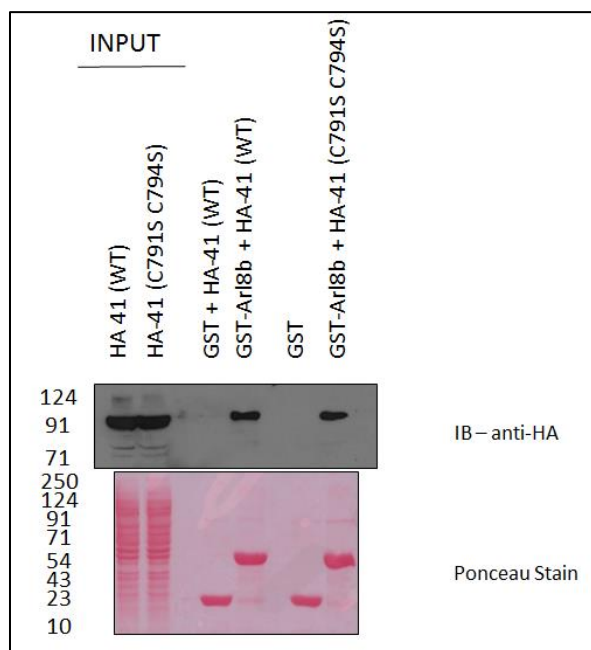


Figure 22. GST Pulldown of HA-tagged Vps41 and HA-tagged Vps41 C791S C794S with GST-tagged Arl8b. GST-Arl8b pulled down HA-tagged Vps41 C791S C794S as strongly as HA-tagged Vps41. The ponceau stain depicts the expression of GST only and GST-Arl8b proteins.

D. hVps41 H819R C822S does not interact with hVps18

H819 and C822 form the part of the first Zinc coordinating site in hVps41 RING apart from C791 and C794. Thus the construct HA-tagged Vps41 H819R C822S was created to compare whether it behaves similar to the Vps41 C791S C794S with respect to the interaction with Vps18. Co-immunoprecipitation analysis showed Vps41-WT dependent immunoprecipitation of Vps18 as expected. However the mutant HA-tagged Vps41 H819R C822S bound Myc-tagged Vps18 weakly; similar to the effect of HA-tagged Vps41 C791S C794S (shown in Figure 23). Thus, the first Zinc coordinating site in Vps41 RING-H2 domain is critical for its interaction with Vps18.

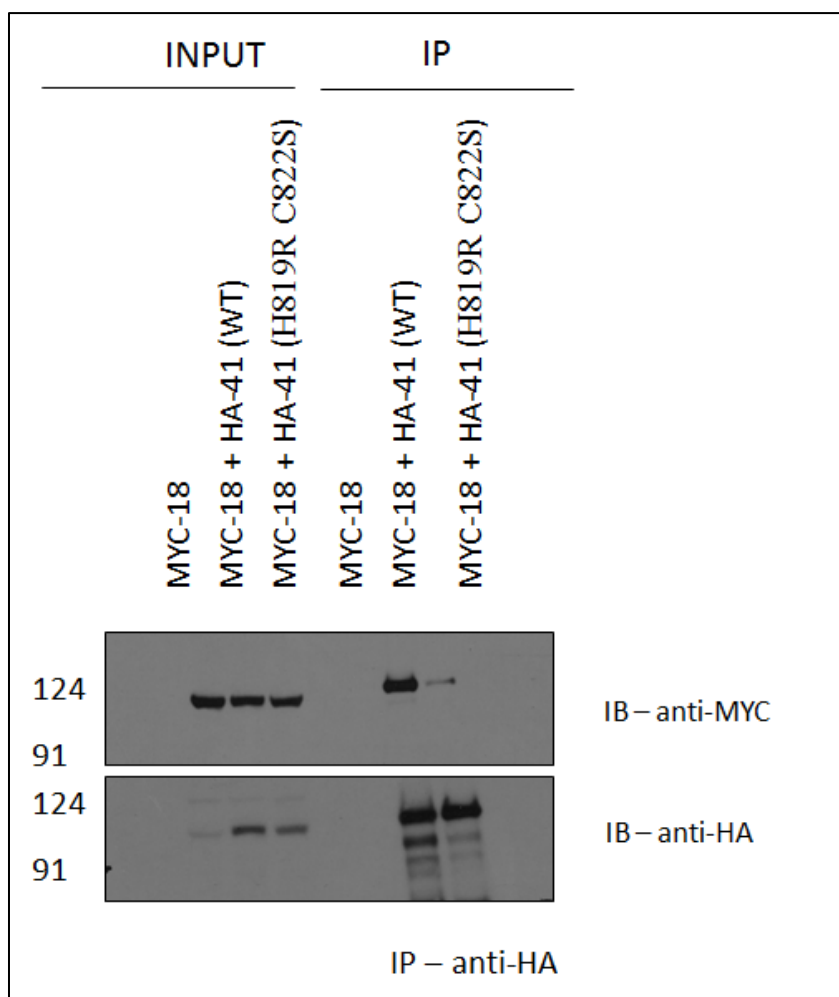


Figure 23. Co-immunoprecipitation of Vps41H819R C822S with Vps18. HEK293T cells were co-transfected with HA-Vps41 H819R C822S and Myc-Vps18. Myc-Vps18 only was a negative control whereas HA-Vps41 WT and Myc-Vps18 was a positive control. Vps18 was pulled down less by the mutant Vps41 H819R C822S compared to Vps41 WT.

2.1.3. The RING domain of Vps18 is essential for its interaction with other HOPS subunits like Vps11, Vps16 and Vps41

Apart from Vps41 subunit, other subunits of HOPS complex like Vps11, Vps16 and Vps18 are known to have RING domain. Since RING-H2 domain of hVps41 is essential for its interaction with hVps18 subunit, we further studied the involvement of RING-H2 domain of hVps18 in the same interaction.

A yeast two hybrid analysis was performed to check the interaction of Vps18 RING domain with other HOPS subunits. To test this, Vps18 WT and Vps18 Δ RING were cloned in fusion with Gal4 binding domain and were used as the bait. The other HOPS subunits were cloned in fusion with Gal4 activation domain. After transformation, yeasts were plated on -2 plate (-Leu -Trp +His) for the confirmation of cotransformants and on -3 plate (-Leu -Trp -His) to detect direct interaction. After 3 to 4 days, Vps18 Δ RING did not show any interaction with Vps41, Vps11 or Vps16 compared to Vps18 WT (shown in Figure 24). The result was reconfirmed by plating on 3-AT (competitive inhibitor of His) which showed an abrogation in the interaction of Vps18 Δ RING with other subunits (shown in Figure 24).

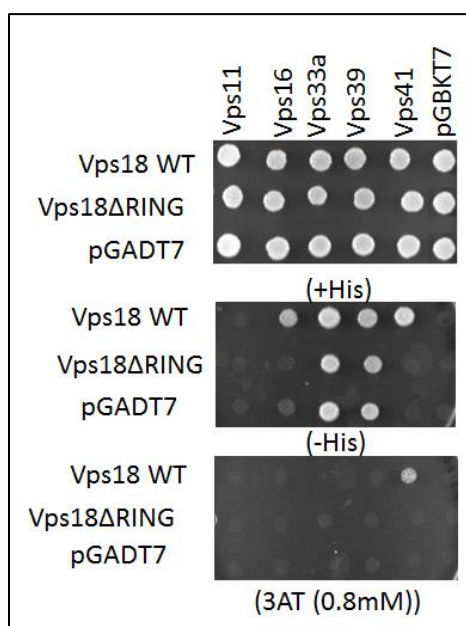


Figure 24. Yeast two hybrid interaction of Vps18 and Vps18 Δ RING (activation domain vector) with other HOPS subunits (binding domain vector) tested using pGBKT7/pGADT7 system. Distinct spots for interaction between Vps18 and Vps41, Vps16, Vps11 were observed. Vps18 Δ RING did not show any interaction.

2.1.4. The cysteine and histidine residues of hVps18 RING domain are involved in its interaction with hVps41

A. hVps18 C853S C856S does not interact with hVps41

C853 and C856 form the part of the first Zinc coordinating site in hVps18 RING and hence the construct Myc-tagged Vps18 C853S C856S was created. We mutated the first two residues of the two Zinc coordinating sites in the RING-H2 domain of Vps18 using site directed mutagenesis. HEK293T cells were co-transfected with HA-tagged Vps41 and Myc-tagged Vps18 C853S C856S subunit of HOPS complex. HEK293T cells were also transfected with HA-tagged Vps41 alone as a negative control and co-transfected with HA-tagged Vps41 subunit and Myc-tagged Vps18 as a positive control. Vps18-WT dependent precipitation of Vps41 was observed as expected. However the mutant Vps18 C853S C856S did not bind HA-tagged Vps41 supported by the absence of band on the blot (shown in Figure 25).

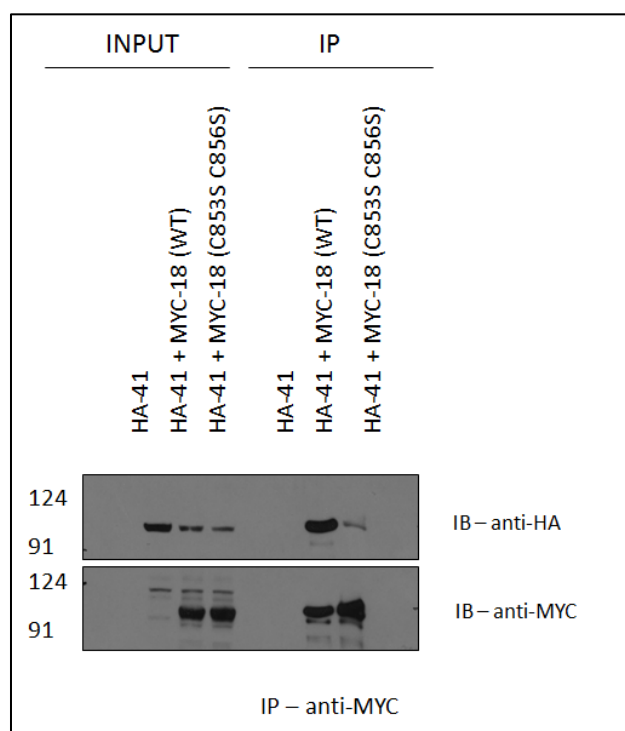


Figure 25. Co-immunoprecipitation of Vps18 C853S C856S (First 2 Cysteines are mutated to Serines) with Vps41. HEK293T cells were cotransfected with Myc-Vps18 C853S C856S and HA-Vps41. Vps41 was pulled down less by Vps18 C853S C856S compared to Vps18 WT.

B. hVps18 C870S H872R interacts weakly with hVps41

C870 and H872 form the part of the second Zinc coordinating site in hVps18 RING. The construct Myc-tagged hVps18 C870S H872R was created to compare functional importance of first and second Zinc coordinating site. HEK293T cells were co-transfected with HA-tagged Vps41 and Myc-tagged Vps18 C870S H872R subunit of HOPS complex. HEK293T cells were also transfected with HA-tagged Vps41 as a negative control and co-transfected with HA-tagged Vps41 subunit and Myc-tagged Vps18 as a positive control. Vps18-WT dependent precipitation of Vps41 was observed as expected. However the mutant hVps18 C870S H872R immunoprecipitated HA-tagged Vps41 weakly compared to Myc-tagged Vps18 WT (shown in Figure 26).

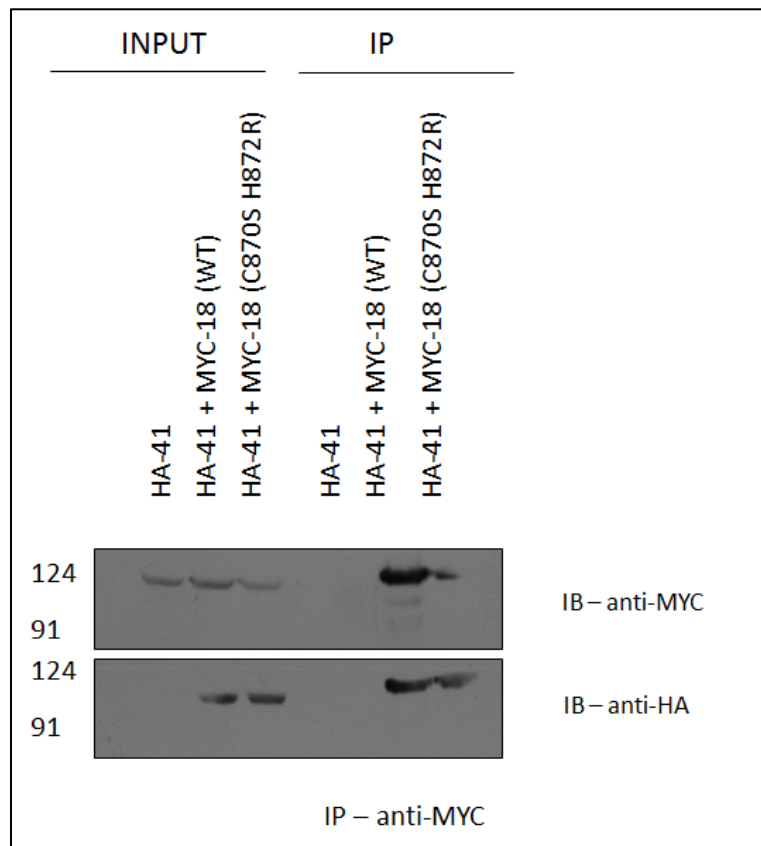


Figure 26. Co-immunoprecipitation of Vps18 C870S H872R (First 2 Cysteines are mutated to Serines) with Vps41. HEK293T cells were cotransfected with Myc-Vps18 C870S H872R and HA-Vps41. Vps41 was pulled down less by Vps18 C870S H872R compared to Vps18 WT.

This proved that cysteine and histidine residues within the RING-H2 domains of Vps41 and Vps18 are critical for their functions and interactions with each other.

2.1.5. Purification of MBP-tagged Vps39 and Vps18 followed by antibody purification

MBP-Vps39 and MBP-Vps18 were purified using the protein purification method under standard conditions mentioned in the methods section. The eluted fractions were passed through the liquid chromatography system AKTA and the purified fractions collected (shown in Figure 27)

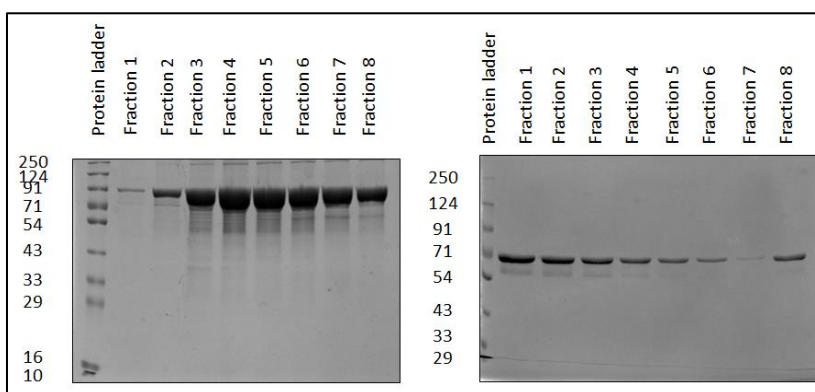


Figure 27. Purified AKTA fractions for MBP-Vps39 and MBP-Vps18. The first figure corresponds to MBP-Vps39 fractions at a size of 85kDa and the second figure corresponds to MBP-Vps18 fractions at a size of 60kDa.

The post-AKTA fractions were further concentrated and compared with Bovine Serum Albumin (BSA) controls for the estimation of concentration (shown in Figure 28). The concentration of MBP-Vps18 was around 4 μg with degradation. MBP-Vps39 concentration was around 2 μg .

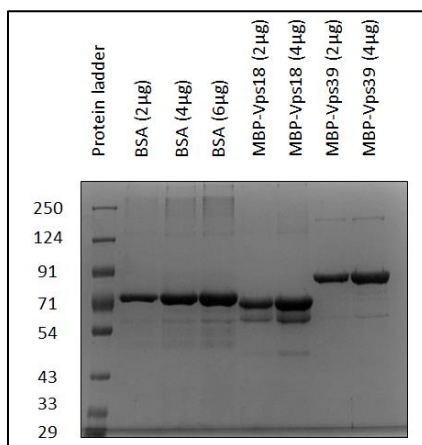


Figure 28. The SDS PAGE gel for purified and concentrated MBP-Vps18 and MBP-Vps39 proteins. The MBP-Vps18 protein shows degradation (presence of double bands). MBP-Vps39 protein product is far stable compared to MBP-Vps18.

The purified proteins were sent for raising antibodies against MBP-Vps39 and MBP-Vps18. These proteins were injected in rabbit and the serum with the raised antibodies was sent to us. The preliminary antibody test with 1:500 dilution of antibodies against MBP-Vps18 and MBP-Vps39 did not show any band at specific size of ~95 KDa (shown in Figure 29).

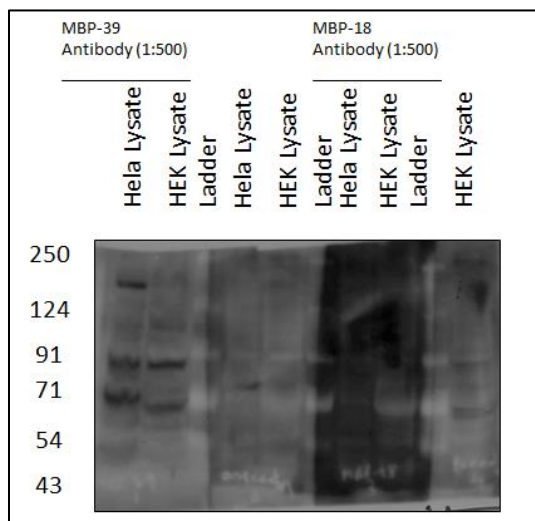


Figure 29. Antibody test for anti MBP-Vps39 and anti MBP-Vps18 proteins. Under 1:500 dilution, both the antibodies failed to detect endogenous expression of Vps39 and Vps18 respectively.

Further, purification of serum containing antibody against MBP-Vps39 was done using Protein G coated beads. This purified antibody failed to detect neither the endogenous Vps39 in HeLa or HEK293T cell lines nor the MBP-tagged Vps39 (shown in Figure 30).

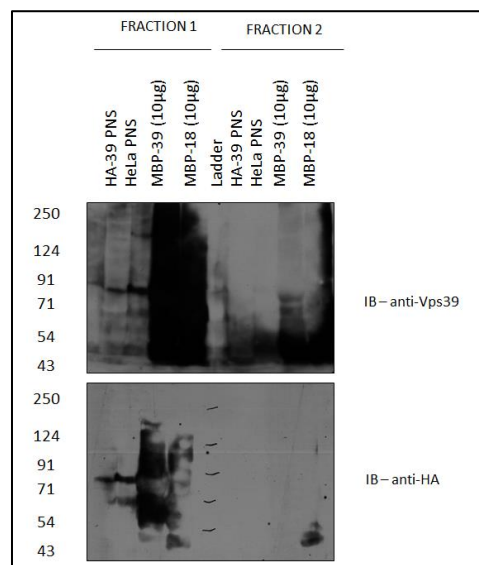


Figure 30. Purification of MBP-Vps39 antibody using Protein G coated beads. The purified antibody fractions failed to detect endogenous expression of Vps39 and the purified proteins.

Vps39-specific antibody was also purified by binding with purified MBP-Vps39 so as to separate out the antibodies that detects the MBP tag or Vps39. The testing with these antibodies was done using HeLa PNS, HA-Vps39 overexpressed HEK293T cells and Vps39 knockdown cells (shown in Figure 31). Again, no specific signal corresponding to the size of Vps39 was observed in these Western blots. Moreover, these antibodies did not detect even the purified protein.

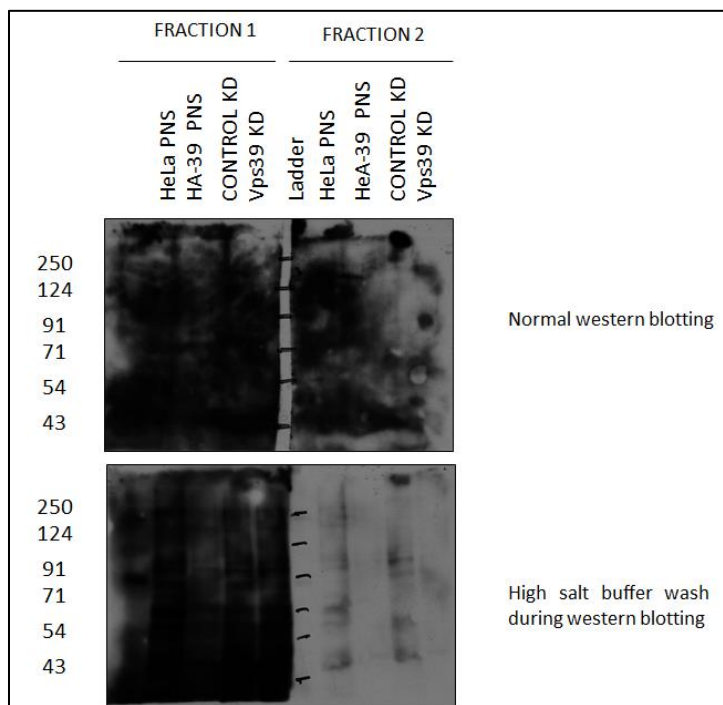


Figure 31. The immunoblot for testing of Rabbit anti MBP-Vps39 synthesized antibody. The antibody was incubated for 2 hours at 1:200 dilution and developed. Further the blot was incubated with the antibody for overnight in 10%skim milk and washed with high salt buffer. Both the immunoblots lack any distinct bands corresponding to detection of Vps39.

2.1.6. Details of cloning done as a part of this project

Table 1. Details of cloning performed as part of MS Thesis project work

| S. No | Insert | Vector | Template | Primer # (MSI-) | Restriction Enzymes |
|-------|-----------------------------------|---------|---|--------------------|------------------------------|
| 1 | Vps41 839X | pCDNA | Vps41 in pCDNA | P15,P16 | EcoRI, HindIII |
| 2 | Vps18 853x | pGADT7 | Vps18 in pGADT7 | 458,459 | EcoRI, BamHI |
| 3 | Vps41 C791S C794S | pCDNA | Vps41 C814S H816R in pCDNA | 481,482 | Site-directed mutagenesis |
| 4 | Vps41 H819R C822S | pCDNA | Vps41 C791S C794S C814S H816R in pCDNA | 483,484 | Site-directed mutagenesis |
| 5 | Vps41 rescue C791S C794S | pCDNA | Vps41 rescue in pCDNA | 481,482 | Site-directed mutagenesis |
| 6 | Vps41 C791S C794S | pGBKT7 | Vps41 in pGBKT7 | 481,482 | EcoRI, HindIII |
| 7 | Vps41 H819R C822S | pCDNA | Vps41 C814S H816R in pCDNA | 483,484 | Site-directed mutagenesis |
| 8 | Vps18 C853S C856S | pCMV | Vps18 in pCMV | 523,524 | Site-directed mutagenesis |
| 9 | HA-Vps41 rescue | pCDH | Vps41 in pCDNA | 505,506 | XbaI, BamHI |
| 10 | Vps41 C791S C794S | pEGFPC1 | Vps41 in pEGFPC1 | 481,482 | EcoRI, HindIII |
| 11 | Vps18 C870S H872R | pCMV | Vps18 in pCMV | 525,526 | Site-directed mutagenesis |
| 12 | HA-Vps41 rescue | pCDH | Vps41 rescue in pCDNA | 481,482 | EcoRI, HindIII |

| | | | | | |
|----|-----------------------------------|---------|--------------------------------------|---------|----------------|
| | C791S C794S | | | | |
| 13 | TAP-Vps41 C791S C794S | pCDH | TAP-Vps41 in pCDH | 481,482 | EcoRI, HindIII |
| 14 | Vps41 RING (713-854) | pEGFPC1 | TAP-Vps41 in pCDH | 82,83 | XhoI, KpnI |
| 15 | Vps41 RING (791-839) | pET15b+ | Vps41 in pCDNA | 528,529 | BamHI, NdeI |
| 16 | Vps18 RING (844-973) | pMALC2x | Vps18 in pCMV | 530,531 | BamHI, SalI |
| 17 | Vps41 rescue | pEGFPC1 | Vps41 rescue in pCDNA | 101,102 | XhoI, BamHI |
| 18 | Vps41 rescue C791S C794S | pEGFPC1 | Vps41 rescue C791S C794S in pCDNA | 101,102 | XhoI, BamHI |

2.2 Future Prospects

In conclusion, we have a Vps41 RING domain mutant that fails to interact with Vps18 and may impair the assembly of HOPS complex on lysosomes. Interestingly, further studies using this RING domain mutant of Vps41 will be fruitful in characterizing the main role of Vps41 in HOPS complex. The future prospects of this study are,

- To assess the assembly of HOPS complex in presence of Vps41 RING domain mutant and compare it to Vps41 WT
- To study cargo trafficking to lysosomes in Vps41-siRNA treated cells expressing either the WT or RING domain mutant of Vps41

These studies will provide an insight to Vps41 mechanism of action and if assembly of the complete HOPS complex is needed for late endosome-lysosome fusion.

Interestingly, an ongoing study from our lab has shown that HOPS complex is essential for *Salmonella typhimurium* replication and survival inside the host. Vps41 C791S C794S domain mutant can be used to study whether it can impair the replication of *S. typhimurium* by blocking the assembly of HOPS complex.

In addition to this, we can delve deep into the functional significance of Vps41 and Vps18 RING domains. The future prospects in this project will be

- To investigate the ubiquitin ligase activity of hVps41 on hVps18 as the substrate.
- hVps18 RING is known to have E3 Ubiquitin ligase activity.
 - Does Vps18 ubiquitinate Vps41?
- Do the Ring Zinc Finger domains of Vps18 and Vps41 interact with each other?

Bibliography

- Balderhaar, H. J. k. and C. Ungermann (2013). "CORVET and HOPS tethering complexes – coordinators of endosome and lysosome fusion." Journal of Cell Science **126**(6): 1307-1316.
- Borden, K. L. (2000). "RING domains: master builders of molecular scaffolds?" J Mol Biol **295**(5): 1103-1112.
- Bröcker, C., A. Kuhlee, et al. (2012). "Molecular architecture of the multisubunit homotypic fusion and vacuole protein sorting (HOPS) tethering complex." Proceedings of the National Academy of Sciences **109**(6): 1991-1996.
- Brzovic, P. S., J. Meza, et al. (1998). "The Cancer-predisposing Mutation C61G Disrupts Homodimer Formation in the NH₂-terminal BRCA1 RING Finger Domain." Journal of Biological Chemistry **273**(14): 7795-7799.
- Burd, C. G., T. I. Strohlic, et al. (2004). "Arf-like GTPases: not so Arf-like after all." Trends in Cell Biology **14**(12): 687-694.
- Duncan, R. and S. C. Richardson (2012). "Endocytosis and intracellular trafficking as gateways for nanomedicine delivery: opportunities and challenges." Mol Pharm **9**(9): 2380-2402.
- Harrington, A. J., T. A. Yacoubian, et al. (2012). "Functional analysis of VPS41-mediated neuroprotection in *Caenorhabditis elegans* and mammalian models of Parkinson's disease." J Neurosci **32**(6): 2142-2153.
- Horazdovsky, B. F., C. R. Cowles, et al. (1996). "A Novel RING Finger Protein, Vps8p, Functionally Interacts with the Small GTPase, Vps21p, to Facilitate Soluble Vacuolar Protein Localization." Journal of Biological Chemistry **271**(52): 33607-33615.
- Huotari, J. and A. Helenius (2011). "Endosome maturation." The EMBO Journal **30**(17): 3481-3500.
- Kaur, G. and S. Subramanian (2015). "A novel RING finger in the C-terminal domain of the coatomer protein α -COP." Biology Direct **10**(1): 1-6.
- Khatter, D., V. B. Raina, et al. (2015). "The small GTPase Arl8b regulates assembly of the mammalian HOPS complex on lysosomes." Journal of Cell Science **128**(9): 1746-1761.
- McVey Ward, D., D. Radisky, et al. (2001). "hVPS41 is expressed in multiple isoforms and can associate with vesicles through a RING-H2 finger motif." Exp Cell Res **267**(1): 126-134.
- Plemel, R. L., B. T. Lobingier, et al. (2011). "Subunit organization and Rab interactions of Vps-C protein complexes that control endolysosomal membrane traffic." Molecular Biology of the Cell **22**(8): 1353-1363.
- Pryor, P. R. and J. P. Luzio (2009). "Delivery of endocytosed membrane proteins to the lysosome." Biochimica et Biophysica Acta (BBA) - Molecular Cell Research **1793**(4): 615-624.
- Rieder, S. E. and S. D. Emr (1997). "A novel RING finger protein complex essential for a late step in protein transport to the yeast vacuole." Mol Biol Cell **8**(11): 2307-2327.
- Ruan, Q., A. J. Harrington, et al. (2010). "VPS41, a protein involved in lysosomal trafficking, is protective in *Caenorhabditis elegans* and mammalian cellular models of Parkinson's disease." Neurobiology of Disease **37**(2): 330-338.

- Saftig, P. and J. Klumperman (2009). "Lysosome biogenesis and lysosomal membrane proteins: trafficking meets function." Nat Rev Mol Cell Biol **10**(9): 623-635.
- Solinger, J. A. and A. Spang (2013). "Tethering complexes in the endocytic pathway: CORVET and HOPS." FEBS Journal **280**(12): 2743-2757.
- van der Kant, R., C. T. H. Jonker, et al. (2015). "Characterization of the Mammalian CORVET and HOPS Complexes and Their Modular Restructuring for Endosome Specificity." Journal of Biological Chemistry **290**(51): 30280-30290.
- van Meel, E. and J. Klumperman (2008). "Imaging and imagination: understanding the endo-lysosomal system." Histochem Cell Biol **129**(3): 253-266.
- Wartosch, L., U. Günesdogan, et al. (2015). "Recruitment of VPS33A to HOPS by VPS16 Is Required for Lysosome Fusion with Endosomes and Autophagosomes." Traffic **16**(7): 727-742.
- Yogosawa, S., S. Hatakeyama, et al. (2005). "Ubiquitylation and degradation of serum-inducible kinase by hVPS18, a RING-H2 type ubiquitin ligase." J Biol Chem **280**(50): 41619-41627.
- Yogosawa, S., M. Kawasaki, et al. (2006). "Monoubiquitylation of GGA3 by hVPS18 regulates its ubiquitin-binding ability." Biochem Biophys Res Commun **350**(1): 82-90.